Journal of Materials Chemistry

Dynamic Article Links

Cite this: *J. Mater. Chem.*, 2011, **21**, 6230

www.rsc.org/materials

**PAPER**

# Transmissive to black electrochromic aramids with high near-infrared and multicolor electrochromism based on electroactive tetraphenylbenzidine units†

**Hung-Ju Yen, Kun-Ying Lin and Guey-Sheng Liou***

***Received 14th January 2011, Accepted 15th February 2011***
**DOI: 10.1039/c1jm10210a**

A series of near-infrared (NIR) electrochromic aromatic polyamides with tetraphenylbenzidine (TPB) units were prepared by phosphorylation polyamidation from a newly synthesized aromatic diamine monomer, *N*,*N*′-bis(4-aminophenyl)-*N*,*N*′-di(4-methoxyphenyl)-4,4′-biphenyldiamine, and various dicarboxylic acids. These polymers were highly soluble in many organic solvents and showed useful levels of thermal stability associated with high glass-transition temperatures and char yields. These anodically polymeric electrochromic materials showed reversible electrochemistry and electrochromism with high contrast ratio both in the visible range and NIR regions. Notably, copolymerization of TPB-based and TPPA-based aramids (TPPA: tetraphenyl-*p*-phenylenediamine) showed a good combination of the individual homopolymers in electrochemical and electrochromic properties, producing a transmissive-to-black electrochromic polymer with high NIR and multicolor electrochromism.

## Introduction

Electrochromic materials exhibit a reversible optical change in absorption or transmittance upon being electrochemically oxidized or reduced, such as transition-metal oxides, inorganic coordination complexes, conjugated polymers, and organic molecules.[1] Despite the fact that the earliest electrochromic devices are mostly based on inorganic oxides, nevertheless, the organic compounds have several advantages over the former ones, such as processability, high coloration efficiency, fast switching ability, and multiple colors within the same material. Initially, investigation of electrochromic materials has been directed towards optical changes in the visible region (*e.g.*, 400–800 nm), proved useful in variable applications such as E-paper, optical switching devices, smart window, and camouflage materials.[2] Increasingly, attention of the optical changes has been extended from the near infrared (NIR; *e.g.*, 800–2000 nm) to the microwave regions of the spectrum, which could be exploitable for optical communication, data storage, and thermal control (heat gain or loss) in buildings and spacecrafts.[3] Therefore, NIR electrochromic materials including transition metal oxides $WO_3$, organic metal complex (ruthenium dendrimers), quinone-containing organic materials, and conjugated polymers have been investigated in recent years.[4] According to Robin and Day,[5] the *N*,*N*,*N*′,*N*′-tetraphenyl-*p*-phenylenediamine (TPPA) cation radical have been reported as a symmetrical delocalized class III structure with a strong electronic coupling, while the *N*,*N*,*N*′,*N*′-tetraphenylbenzidine (TPB) cation radical was demonstrated as a class II structure with a weakly electronic coupling, both leading intervalence charge transfer (IV-CT) absorption bands in the NIR region.[6] These results made aryldiamine-containing molecules an interesting anodic electrochromic system for NIR applications.

Since 2005, our group has reported several arylamine/triphenylamine (TPA) containing electrochromic polymers (ECPs) with interesting color transitions and good electrochromic reversibility in the visible region or NIR range,[7] which could be differentiated on the method of increasing coloring stages. A first class spans materials polymerized from two electroactive monomers (*e.g.*, polyamides prepared by electroactive diamines and diacids).[7a–7d] A second class includes the further chemical modification of electroactive units on the end functional groups of electrochromic hyperbranched polymers.[7e] A third class is represented by increasing the electroactive sites into the synthesized monomers by multi-step procedure approaches.[7f,7g] In addition, it is also important to note that most of the colors in the visible spectrum can be attained with red,[8] green[9] and blue[10] ECPs according to color mixing theory, which claims that if two colors are mixed, the resulting color will lie somewhere along a straight line connecting two points on the chromaticity diagram.[1i] To date, significant efforts have been devoted to the design and synthesis of novel ECPs with saturated and tunable colors. In spite of the panoramic breadth of the colors of ECPs,

*Functional Polymeric Materials Laboratory, Institute of Polymer Science and Engineering, National Taiwan University, 1 Roosevelt Road, 4th Sec., Taipei, 10617, Taiwan. E-mail: gsliou@ntu.edu.tw*

† Electronic supplementary information (ESI) available: A movie of electrochromic switches between neutral and oxidation states (AVI). Tables: inherent viscosity, molecular weights, solubility behavior, and thermal properties. Figures: NMR of monomers, IR of monomers and polyamide, TGA and DSC traces of polyamides. See DOI: 10.1039/c1jm10210a

the construction of a transmissive-to-black ECP remains elusive due to the complexity of designing such material, which is also a challenging task to access in view of optoelectronic devices. Therefore, our strategy is to design and synthesize TPB-based ECPs with a longer distance between two electroactive nitrogen centers and higher absorption wavelength than the TPPA-based ones.[6b] Furthermore, by the copolymerization of these two ECPs, the absorbing bands and reflected coloration could be merged and offer the potential for ECPs possessing either highly saturated or darker colors.

In this contribution, we synthesized the TPB-based diamine monomer, *N*,*N*′-bis(4-aminophenyl)-*N*,*N*′-di(4-methoxyphenyl)-4,4′-biphenyldiamine, and its derived aromatic polyamides containing *para*-substituted methoxy groups which could not only enhance the solubility by a high steric hindrance for close packing but also greatly prevent the electrochemical coupling reactions by affording stable cationic radicals. The result TPB-based polyamides are expected to reveal a slightly bathochromic shift when compared with the reported TPPA-based ones in the oxidized stages due to the longer conjugating length between two electroactive nitrogen atoms. In addition, by random copolymerization of TPB and TPPA-based diamine monomers, the resulting copolymer **IIb** could exhibit extensive absorption ranging of 400–750 nm required for a black electrochromism in the oxidized state.

## Results and discussion

### Monomer and polymer synthesis

The new diamine with TPB unit, *N*,*N*′-bis(4-aminophenyl)-*N*,*N*′-di(4-methoxyphenyl)-4,4′-biphenyldiamine (**2**), was synthesized by palladium catalyzed hydrazine reduction of *N*,*N*′-bis(4-nitrophenyl)-*N*,*N*′-di(4-methoxyphenyl)-4,4′-biphenyldiamine (**1**) resulting from the Cu-mediated Ullmann condensation of 4-methoxy-4′-nitrodiphenylamine and 4,4′-diiodo-biphenyl (Scheme 1). Elemental analysis, FT-IR, and NMR spectroscopic techniques were used to identify structures of the intermediate dinitro compound **1** and the target diamine monomer **2**. The $^{1}$H NMR and $^{13}$C NMR spectra of the diamine monomer **2** are illustrated in the ESI (Fig. S1 to S4)† and agree well with the proposed molecular structures. Thus, the results of all the spectroscopic and elemental analyses suggest the successful preparation of the target diamine monomer.

According to the phosphorylation technique first described by Yamazaki and co-workers,[11] two series of novel polyamides **I** and **I**′ were synthesized from the diamine monomer **2** and **2**′ and three commercial dicarboxylic acids **3a–3c**. On the other hand, copolymer **IIb** was prepared from TPB-based diamine **2** and TPPA-based diamine **2**″ (Scheme 2). The polymerization was carried out *via* solution polycondensation using triphenyl phosphite and pyridine as condensing agents. All polymerization reactions proceeded homogeneously and gave high molecular weights. The obtained polyamides had inherent viscosities in the

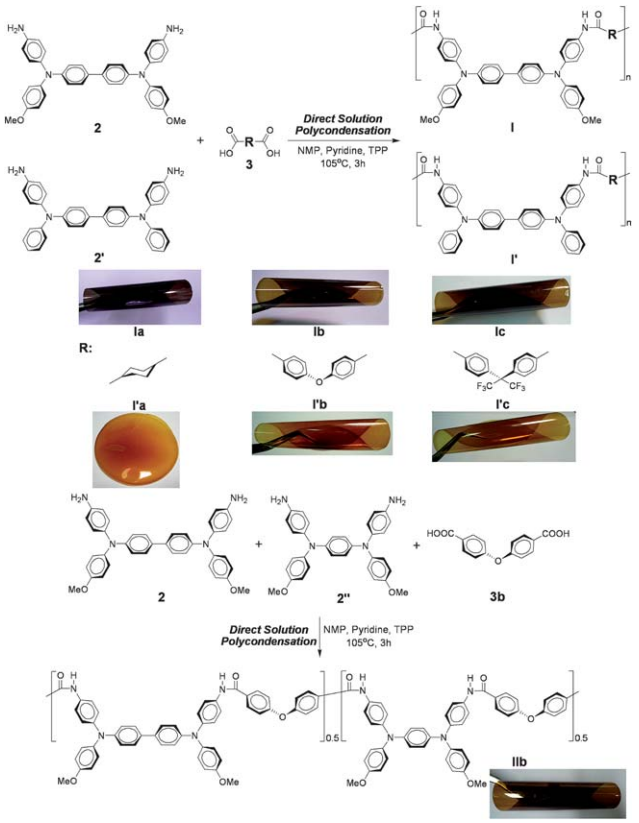


**Scheme 2** Synthesis of aromatic polyamides **I**, **I**′, and **IIb**. The photographs show the appearance of the flexible films (thickness: 75–100 μm).

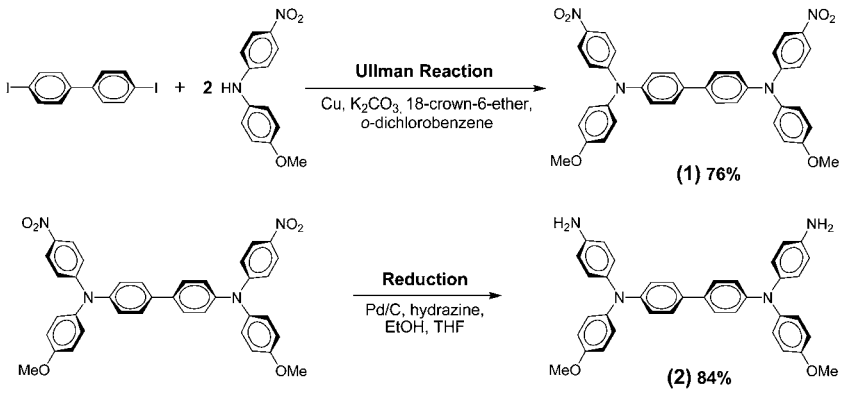


**Scheme 1** Synthetic route to TPB-based diamine monomer **2**.

range of 0.42–0.91 dL/g with weight-average molecular weights ($M_w$) and polydispersity (PDI) of 45 800–125 600 daltons and 1.41–1.89, respectively, relative to polystyrene standards (Table S1).† All the high molecular weights polymers could be cast into transparent, flexible, and tough films *via* solution casting. The appearance and quality of these films are also shown in Scheme 2. The structures of the polyamides were confirmed by elemental analysis and IR spectroscopy. As shown in Figure S5,† a typical IR spectrum for polyamide **Ib** exhibited characteristic IR absorption bands of the amide group around 3315 (N–H stretching) and 1660 $cm^{-1}$ (amide carbonyl).

### Solubility and film properties

The solubility properties of polymers were investigated at 0.5% w/v concentration and the results are listed in Table S2.† Most of the polyamides were readily soluble in polar aprotic organic solvents such as *N*-methyl-2-pyrrolidinone (NMP), *N*,*N*-dimethylacetamide (DMAc), *N*,*N*-dimethylformamide (DMF), and *m*-cresol. The polyamides **I** had higher solubility than **I′**, which could be attributed to the introduction of the bulky pendent 4,4′-dimethoxy-substituted TPB moiety into the repeat unit. The excellent solubility makes these polymers as potential candidates for practical applications by spin-coating or inkjet-printing processes to afford high performance thin films for optoelectronic devices.

The thermal properties of polyamides were examined by TGA and DSC, and the data are summarized in Table S3.† Typical TGA curves of representative polyamides **Ib** and **I′b** in both air and nitrogen atmospheres are shown in Figure S6.† All the prepared polyamides exhibited good thermal stability with insignificant weight loss up to 450 °C under nitrogen or air atmosphere even with the introduction of methoxy groups. The 10% weight loss temperatures of these polymers in nitrogen and air were recorded in the range of 475–585 and 490–570 °C, respectively. The carbonized residue (char yield) of these polymers in a nitrogen atmosphere was more than 53% at 800 °C. The high char yields of these polymers can be ascribed to their high aromatic content. The glass-transition temperatures ($T_g$) of these polyamides could be easily measured by the DSC thermograms; they were observed in the range of 270–315 °C (as shown in Figure S7),† depending upon the stiffness of the polymer chain.

### Electrochemical properties

The redox behavior of the polyamides were investigated by cyclic voltammetry (CV) and differential pulse voltammetry (DPV) conducted by the cast film on an indium-tin oxide (ITO) coated glass slide as working electrode in anhydrous acetonitrile ($CH_3CN$), using 0.1 M of tetrabutylammonium perchlorate (TBAP) as a supporting electrolyte under a nitrogen atmosphere. The typical CV for polyamides **Ib** (with 4,4′-dimethoxy-substituted) and **I′b** (without 4,4′-dimethoxy-substituted) are shown in Fig. 1a for comparison. We observe two reversible oxidation redox steps for polyamides **Ib** and **I′b**, which means that electrons are successively removed from the two different redox centers and a higher potential is needed to transform $\mathbf{Ib}^+$ into $\mathbf{Ib}^{2+}$. The lower oxidation potential and higher electrochemical stability of polyamide **Ib** comparing to its analog **I′b** could be attributed to

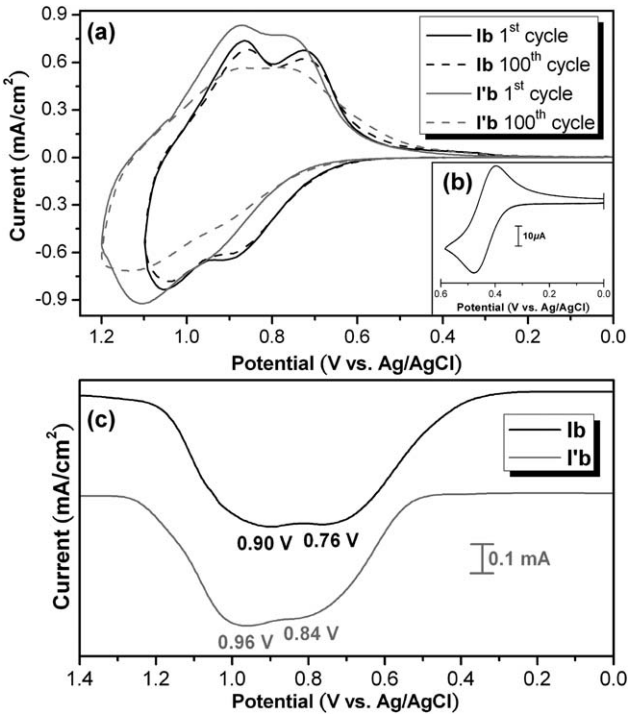


**Fig. 1** Cyclic voltammetric diagrams of (a) polyamide **Ib** and **I′b** films on an ITO-coated glass substrate over cyclic scans and (b) ferrocene (inset) in 0.1 M TBAP/$CH_3CN$ at a scan rate of 50 mV/s, and (c) differential pulse voltammograms of polymer **Ib** and **I′b** films onto an ITO-coated glass substrate in 0.1 M TBAP/$CH_3CN$. Scan rate, 5 mV/s; pulse amplitude, 50 mV; pulse width, 50 ms; pulse period, 0.2 s.

the *para*-position substituted methoxy group on TPB groups. Moreover, the DPV clearly showed two splitting oxidation potentials for polyamide **Ib** (0.76 and 0.90 V) and **I′b** (0.84 and 0.96 V) (as shown in Fig. 1c), suggesting charge delocalization through the biphenyl unit in its mixed-valence $\mathbf{Ib}^+$ and longer distance electronic coupling between the bridged of TPB moieties. During the electrochemical oxidation of the polyamide thin films, the color of the film changed from colorless to red brown and then to blue. The other polyamides showed similar CV curves to Fig. 1. The redox potentials of the polyamides as well as their respective highest occupied molecular orbital (HOMO) and lowest unoccupied molecular orbital (LUMO) (*versus* vacuum) are shown in Table 1. The HOMO level or called ionization potentials (*versus* vacuum) of polyamides **Ia–Ic** are estimated from the onset of their oxidation in CV experiments as 5.05–5.06 eV (on the basis that ferrocene/ferrocenium is 4.8 eV below the vacuum level with $E_{onset} = 0.36$ V).

In addition, Fig. 2 shows the CV and DPV of copolymer **IIb** and the corresponding individual molecular structure of **Ib** and **I″b**. Due to the lack or absence of electrochemical splitting for the $\mathbf{IIb}^{3+}$ and $\mathbf{IIb}^{4+}$ resulted from cationic radical of $\mathbf{Ib}^+$ and $\mathbf{I''b}^+$, respectively, the separation was further investigated by spectrochemical UV-Vis-NIR investigations.

### Spectroelectrochemistry

Spectroelectrochemical experiments were used to evaluate the optical properties of the electrochromic films. For the

 

**Table 1** Redox Potentials and Energy Levels of Polyamides

| | Thin films (nm) | | Oxidation potential (V)[a] | | | | | |
|---|---|---|---|---|---|---|---|---|
| | | | $E_{1/2}$ | | | | | |
| Polymer | $\lambda_{max}$ | $\lambda_{onset}$ | 1st | 2nd | $E_{onset}$ | $E_g$ (eV)[b] | HOMO (eV)[c] | LUMO (eV) |
| **Ia** | 312 | 399 | 0.72 | 0.88 | 0.61 | 3.11 | 5.05 | 1.94 |
| **Ib** | 342 | 411 | 0.74 | 0.89 | 0.61 | 3.02 | 5.05 | 2.03 |
| **Ic** | 308 | 415 | 0.76 | 0.92 | 0.62 | 2.99 | 5.06 | 2.07 |
| **I′b** | 341 | 402 | 0.80 | 0.95 | 0.70 | 3.08 | 5.14 | 2.06 |

[a] From cyclic voltammograms *versus* Ag/AgCl in $CH_3CN$. $E_{1/2}$: Average potential of the redox couple peaks. [b] The data were calculated from polymer films by the equation: $E_g = 1240/\lambda_{onset}$ (energy gap between HOMO and LUMO). [c] The HOMO energy levels were calculated from cyclic voltammetry and were referenced to ferrocene (4.8 eV; onset = 0.36 V).

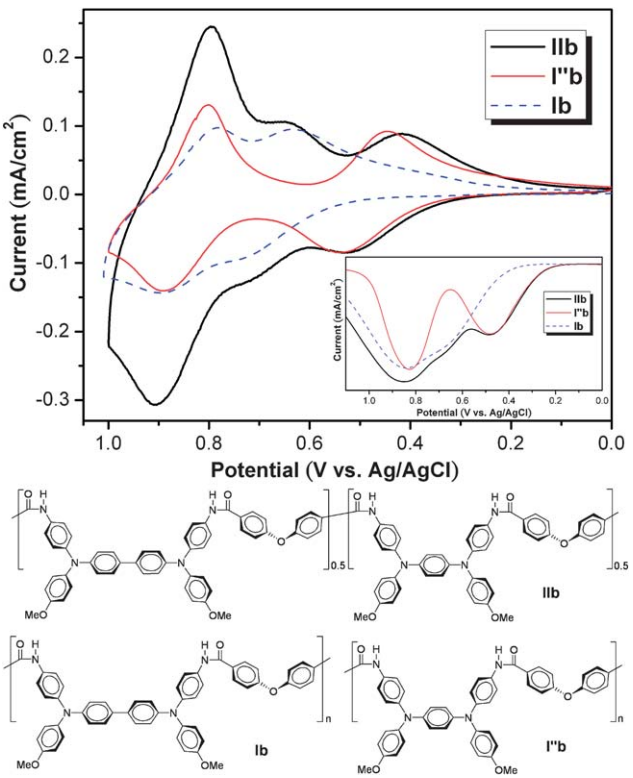


**Fig. 2** Cyclic voltammetric diagrams of polyamide **IIb**, **Ib** and **I′′b** films on an ITO-coated glass substrate in 0.1 M TBAP/$CH_3CN$ at a scan rate of 5 mV/s, and differential pulse voltammograms (inset) of polymer films onto an ITO-coated glass substrate in 0.1 M TBAP/$CH_3CN$. Scan rate, 1 mV/s; pulse amplitude, 50 mV; pulse width, 50 ms; pulse period, 0.2 s.

investigations, the polyamide film was cast on an ITO-coated glass slide, and a homemade electrochemical cell was built from a commercial ultraviolet (UV)-visible cuvette. The cell was placed in the optical path of the sample light beam in a UV-Vis-NIR spectrophotometer, which allowed us to acquire electronic absorption spectra under potential control in a 0.1 M TBAP/$CH_3CN$ solution. UV-Vis-NIR absorbance curves correlated to applied potentials and three-dimensional transmittance–wavelength–applied potential correlation of **Ib** film are depicted in Fig. 3.

In the neutral form (0 V), the colorless **Ib** film exhibited strong characteristic absorption at 357 nm of triarylamine in the visible region. Upon oxidation (increasing applied voltage from 0 to 0.80 V), the intensity of the absorption peak at 357 nm gradually decreased while a new peak at 486 nm and a broad IV-CT band centered around 1350 nm in the NIR region gradually increased in intensity. We attribute the spectral change in visible light region to the formation of a stable monocation radical of the TPA center in TPB moiety. Furthermore, the broad absorption in NIR region was the characteristic result due to IV-CT excitation between states in which the positive charge is centered at different nitrogen atoms, which was consistent with the phenomenon classified by Robin and Day.[5] As the more anodic potential to 1.05 V, the absorption bands of the cation radical decreased gradually with a new broad band centered at around 954 nm. The disappearance of NIR absorption band can be attributed to the further oxidation from monocation radical species to the formation of dication in the TPB segments. The UV-Vis-NIR absorption changes in the polyamide **Ib** film at various potentials were fully reversible associated with strong color changes. The other polyamides showed similar spectral change to that of **Ib**. From the inset shown in Fig. 3, the polyamide **Ib** film switches from a transmissive neutral state (colorless; $L^*$, 96.0; $a^*$, −0.4; $b^*$, −0.1) to a highly coloring semi-oxidized state (red-brown; $L^*$, 54.9; $a^*$, 21.6; $b^*$, 25.1) and a fully oxidized state (deep blue; $L^*$, 50.5; $a^*$, −13.4; $b^*$, −8.6). The colorations were homogeneously distributed across the polymer film and survived for more than hundreds of redox cycles. The polymer **Ib** showed good contrast both in the visible and NIR regions with a high optical transmittance change ($\Delta\%T$) of 46% at 1350 nm for red brown coloring at the first oxidation stage, and 88% at 954 nm for blue coloring at the second oxidation stage.

UV-Vis-NIR absorbance curves correlated to applied potentials of copolymer **IIb** film are summarized in Fig. 4 and compared with the corresponding molecular structure of **Ib** and **I′′b** films (Fig. 5). This nearly colorless film exhibited a strong band at 351 nm in the neutral form. Upon oxidation of the **IIb** film (increasing electrode potential from 0 to 0.60 V), the intensity of the absorption bands at 351 nm gradually decreased while new peaks at 433 and 1080 nm gradually increased in intensity due to the formation of cation radical **IIb**$^+$ (Fig. 4a), which is corresponding to the spectral changes of **I′′b**$^+$. Meanwhile, the color of the film changed from colorless ($L^*$, 96.0; $a^*$, −0.4; $b^*$, −0.2) to green ($L^*$, 68.7; $a^*$, −14.0; $b^*$, −17.5). The **IIb**$^{2+}$, appearing at potentials between 0.60 and 0.80 V, exhibited two new shoulders at 486 and 749 nm with a broad absorption from

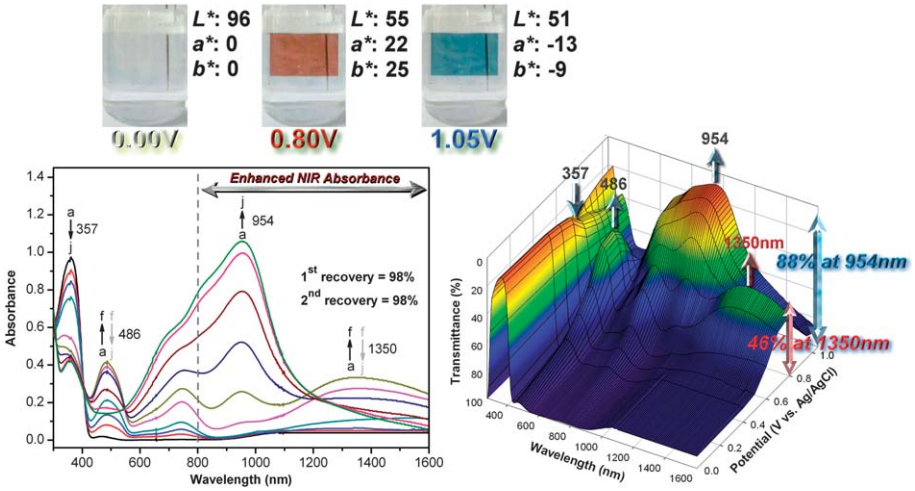


**Fig. 3** Electrochromic behavior (left) at applied potentials of (a) 0.00, (b) 0.4, (c) 0.5, (d) 0.6, (e) 0.7, (f) 0.8, (g) 0.85, (h) 0.9, (i) 0.95, (j) 1.05 (V *vs.* Ag/AgCl), and 3-D spectroelectrochemical behavior (right) from 0.00 to 1.05 (V *vs.* Ag/AgCl) of a polyamide **Ib** thin film (~65 nm in thickness) on the ITO-coated glass substrate in 0.1 M TBAP/$CH_3CN$, the recovery was the absorbance ratio of the neutral state to the cation state for the 1st and the dication state for the 2nd at 357 nm.

800 nm to 1600 nm in the NIR region, which were consistent with the absorption of $\mathbf{Ib}^{+}$. As shown in Fig. 4b and 5a, the $\mathbf{IIb}^{2+}$ is nearly black in color ($L^*$, 58.2; $a^*$, 3.1; $b^*$, 3.2) and revealed a broad visible absorption from 450 to 700 nm with a good combination of the NIR absorption. The colorimetric result is consistent with the absorption spectra of $\mathbf{IIb}^{2+}$ thin film (Fig. 4b) as a small amount of red and yellow light is transmitted. By further applying positive potential value up to 0.90 V

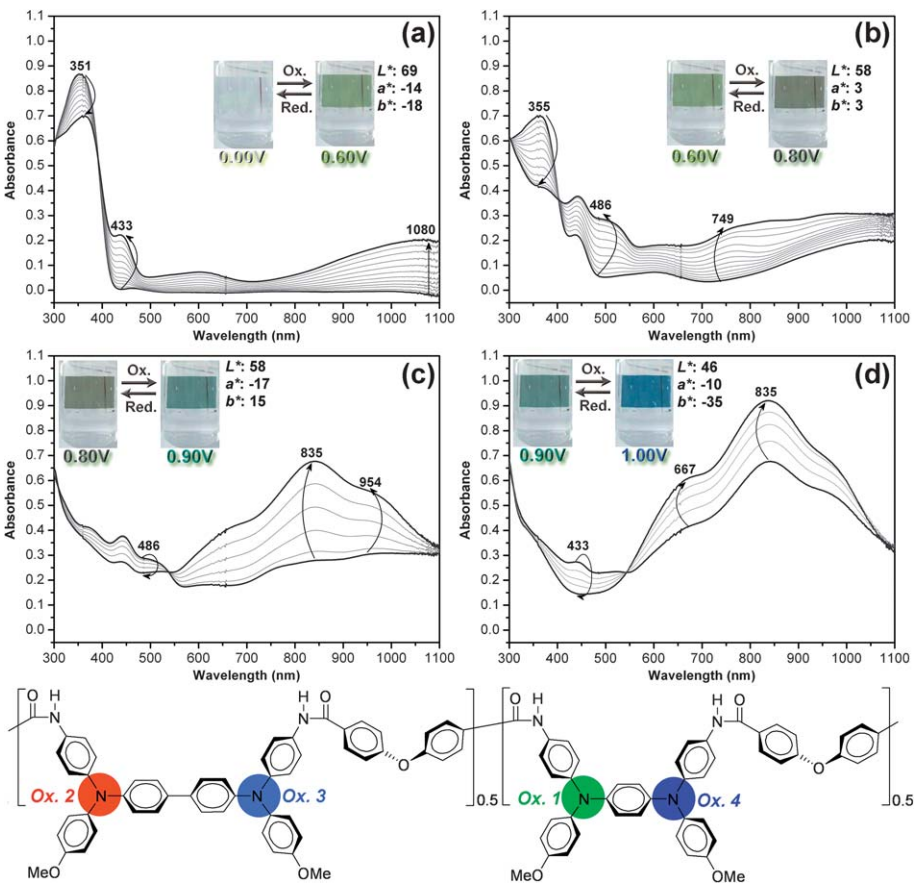


**Fig. 4** Spectroelectrochemistry of polyamide **IIb** thin film (~65 nm in thickness) on an ITO-coated glass substrate in 0.1 M TBAP/$CH_3CN$ by increasing the applied voltage to (a) 0.60, (b) 0.80, (c) 0.90, and (d) 1.00 (V *vs.* Ag/AgCl) and the possible electro-oxidation order for the amino centers. The potential was varied in 25 mV intervals. The inset shows the color change of the polymer film at the indicated potentials.

 

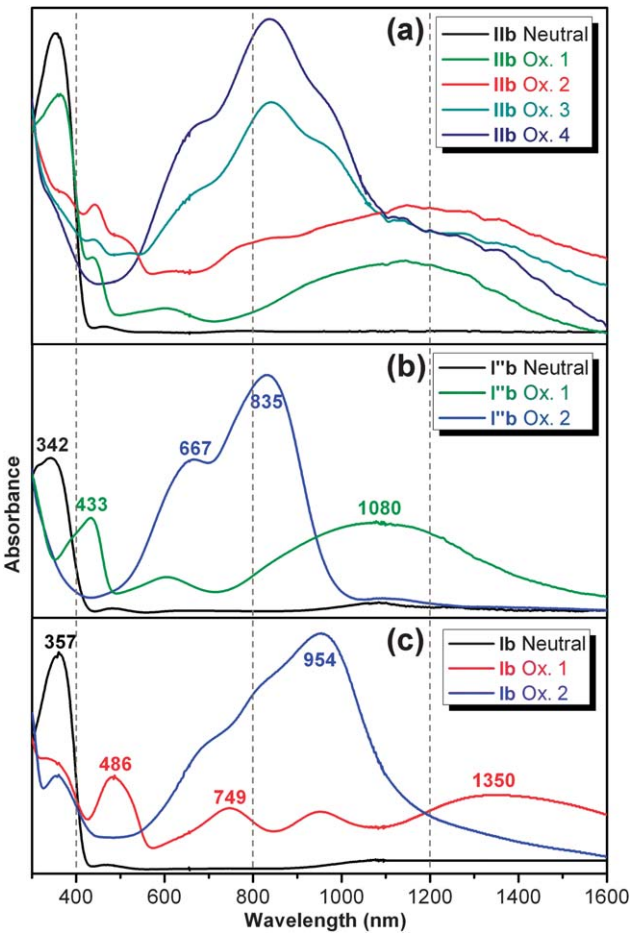


**Fig. 5** Spectroelectrochemistry of polyamides (a) **IIb**, (b) **I′′b** and (c) **Ib** thin films on an ITO-coated glass substrate in 0.1 M TBAP/$CH_3CN$ as their neutral and oxidized forms.

corresponding to $\mathbf{IIb}^{3+}$, the characteristic absorbance at 835 and 954 nm appeared with an absence of the shoulder at 486 nm. Therefore, the spectral change of $\mathbf{IIb}^{3+}$ could be attributed to the oxidation of $\mathbf{Ib}^{+}$ species to the formation of $\mathbf{Ib}^{2+}$ in the TPB segments, and the film became a bluish-green color ($L^*$, 57.7; $a^*$, −16.7; $b^*$, 14.7) during the third oxidation. When the applied potential was added to 1.00 V, the absorption bands at 433 nm decreased gradually with a new shoulder at 667 nm and agree well with the spectral change of $\mathbf{I''b}^{2+}$. At the final stage, the polymer film turned to a deep blue color ($L^*$, 45.7; $a^*$, −10.1; $b^*$, −35.0). The results demonstrated a new approach for tuning the absorption regions not only the coloration changed in visible region but also in the NIR range.

## Conclusions

A series of UV-Vis-NIR electrochromic aromatic polyamides with TPB units were readily prepared *via* phosphorylation polyamidation. In addition to high $T_g$ and good thermal stability, all the obtained polymers also reveal valuable electrochromic characteristics such as high contrast in UV-Vis-NIR region and good electrochromic/electroactive reversibility. Moreover, a novel solution-processable transmissive-to-black electrochromic copolymer also could be obtained from the TPPA-based diamine and newly synthesized TPB-based diamine. Our simple band-merging concept is an effective approach to generate electroactive polymers which are colorless in neutral state, but with which broad and homogeneous absorption bandwidths extending over the entire visible spectrum could be successfully achieved during different oxidation stages that will span numerous applications including electrochromic windows and displays.

## Experimental

### Materials

*N*,*N*′-Bis(4-aminophenyl)-*N*,*N*′-diphenyl-4,4′-biphenyldiamine[12] (**2′**), *N*,*N*′-bis(4-aminophenyl)-*N*,*N*′-di(4-methoxylphenyl)-1,4-phenylenediamine[10i] (**2′′**), and 4-methoxy-4′-nitrodiphenylamine[7f] were synthesized according to a previously reported procedure. Commercially available dicarboxylic acids such as trans-1,4-cyclohexanedicarboxylic acid (**3a**), 4,4′-oxydibenzoic acid (**3b**), and 2,2-bis(4-carboxyphenyl)hexafluoropropane (**3c**) were purchased from Tokyo Chemical Industry (TCI) Co. and used as received. Commercially obtained anhydrous calcium chloride ($CaCl_2$) was dried under vacuum at 180 °C for 8 h. TBAP (ACROS) was recrystallized twice by ethyl acetate under nitrogen atmosphere and then dried *in vacuo* prior to use. All other reagents were used as received from commercial sources.

### *N*,*N*′-Bis(4-nitrophenyl)-*N*,*N*′-di(4-methoxylphenyl)-4,4′-biphenyldiamine (1)

To a solution of 2.03 g (5.00 mmol) of 4,4′-diiodo-biphenyl, 2.93 g (12.00 mmol) of 4-methoxy-4′-nitrodiphenylamine, 3.08 g (22.30 mmol) of powdered anhydrous potassium carbonate, 1.42 g (22.30 mmol) of copper powder and 0.66 g (2.50 mmol) of 18-crown-6-ether was stirred in 10 mL of *o*-dichlorobenzene under nitrogen atmosphere. After being heated at 180 °C for 24 h, the solution was filtered and cooled to precipitate brown crystals. The precipitated brown crystals were collected by filtration and purified by *o*-dichlorobenzene/ethyl acetate. The product was filtered to afford 3.19 g (76% in yield) of brown crystals with a mp of 202–203 °C (by Melting Point System at a scan rate of 1 °C/min). $^1$H NMR (500 MHz, DMSO-$d_6$, δ, ppm): 3.79 (s, 6H, -$OCH_3$), 6.82 (d, $J$ = 9.3 Hz, 4H, $H_d$), 7.05 (d, $J$ = 8.8 Hz, 4H, $H_f$), 7.26 (d, $J$ = 8.8 Hz, 4H, $H_e$), 7.32 (d, $J$ = 8.5 Hz, 4H, $H_b$), 7.72 (d, $J$ = 8.5 Hz, 4H, $H_a$), 8.07 (d, $J$ = 9.3 Hz, 4H, $H_c$). $^{13}$C NMR (125 MHz, DMSO-$d_6$, δ, ppm): 55.3, 115.5, 116.2, 125.6, 126.4, 128.0, 128.9, 136.4, 137.3, 138.6, 144.3, 153.4, 157.7. Anal. Calcd (%) for $C_{38}H_{30}N_4O_6$ (638.7): C, 71.46; H, 4.73; N, 8.77. Found: C, 70.83; H, 4.67; N, 8.43. ESI-MS: calcd for $(C_{38}H_{30}N_4O_6)^+$: m/z 638.7; found: m/z 638.0.

### *N*,*N*′-Bis(4-aminophenyl)-*N*,*N*′-di(4-methoxylphenyl)-4,4′-biphenyldiamine (2)

In a 100 mL three-neck round-bottomed flask equipped with a stirring bar under nitrogen atmosphere, 1.28 g (2.00 mmol) of dinitro compound **1** and 0.1 g of 10% Pd/C were dispersed in 10 mL of ethanol and 25 mL of THF. The suspension solution

was heated to reflux, and 1 mL of hydrazine monohydrate was added slowly to the mixture. After a further 30 h of reflux, the solution was filtered to remove Pd/C, and the filtrate was cooled under nitrogen atmosphere. The precipitated product was collected by filtration and dried *in vacuo* at 80 °C to give 0.93 g (84% in yield) of light green powder with a mp of 190–191 °C (by Melting Point System at a scan rate of 1 °C/min). FT-IR (KBr): 3430, 3350 $cm^{-1}$ (N-H stretch). $^1H$ NMR (500 MHz, DMSO-$d_6$, δ, ppm): 3.72 (s, 6H, -$OCH_3$), 5.01 (s, 4H, -$NH_2$), 6.56 (d, $J = 8.3$ Hz, 4H, $H_c$), 6.74 (d, $J = 8.5$ Hz, 4H, $H_b$), 6.82 (d, $J = 8.3$ Hz, 4H, $H_d$), 6.87 (d, $J = 8.7$ Hz, 4H, $H_e$), 7.00 (d, $J = 8.7$ Hz, 4H, $H_f$), 7.34 (d, $J = 8.5$ Hz, 4H, $H_a$). $^{13}C$ NMR (125 MHz, DMSO-$d_6$, δ, ppm): 55.1, 114.6, 114.8, 118.6, 125.7, 126.2, 127.4, 130.8, 135.5, 140.5, 145.8, 147.4, 155.1. Anal. Calcd (%) for $C_{38}H_{34}N_4O_2$ (578.7): C, 78.87; H, 5.92; N, 9.68. Found: C, 78.46; H, 5.88; N, 10.01. ESI-MS: calcd for $(C_{38}H_{34}N_4O_2)^+$: m/z 578.7; found: m/z 578.4.

### Polymer synthesis

The synthesis of polyamide **Ib** was used as an example to illustrate the general synthetic route utilized to produce the polyamides. A mixture of 578.7 mg (1.00 mmol) of the diamine monomer **2**, 259.1 mg (1.00 mmol) of 4,4′-oxydibenzoic acid (**3b**), 100 mg of calcium chloride, 0.80 mL of triphenyl phosphite, 0.40 mL of pyridine, and 0.80 mL of NMP was heated with stirring at 105 °C for 3 h. The obtained polymer solution was poured slowly into 300 mL of stirred methanol giving rise to a stringy, fiber-like precipitate that was collected by filtration, washed thoroughly with hot water and methanol, and dried under vacuum at 100 °C. Reprecipitations of the polymer by *N*, *N*-dimethylacetamide (DMAc)/methanol were carried out twice for further purification. The inherent viscosity and weight-average molecular weights ($M_w$) of the obtained polyamide **Ib** were 0.76 dL/g (measured at a concentration of 0.5 g/dL in DMAc at 30 °C) and 94 600 daltons, respectively. The FT-IR spectrum of **Ib** (film) exhibited characteristic amide absorption bands at 3315 $cm^{-1}$ (N–H stretch), 3045 $cm^{-1}$ (aromatic C–H stretch), 2935, 2835 $cm^{-1}$ ($CH_3$ C–H stretch), 1660 $cm^{-1}$ (amide carbonyl), Anal. Calcd (%) for $(C_{54}H_{46}N_4O_5)_n$ $(830.97)_n$: C, 78.05; H, 5.58; N, 6.74. Found: C, 76.60; H, 4.96; N, 6.93. The other polyamides were prepared by an analogous procedure.

### Preparation of the polyamide films

A solution of the polymer was made by dissolving about 0.5 g of the polyamide sample in 10 mL of DMAc or NMP. The homogeneous solution was poured into a 9 cm glass Petri dish, which was placed in a 90 °C oven for 5 h to remove most of the solvent; then the semi-dried film was further dried *in vacuo* at 170 °C for 8 h. The obtained films were about 75–100 μm thick and were used for solubility tests, and thermal analyses.

### Measurements

Fourier transform infrared (FT-IR) spectra were recorded on a PerkinElmer Spectrum 100 Model FT-IR spectrometer. Elemental analyses were run in a Heraeus VarioEL-III CHNS elemental analyzer. NMR spectra were measured on a Bruker Avance-500 MHz spectrometer in DMSO-$d_6$, using tetramethylsilane as an internal reference, and peak multiplicity was reported as follows: s, singlet; d, doublet. The inherent viscosities were determined at 0.5 g/dL concentration using a Tamson TV-2000 viscometer at 30 °C. Gel permeation chromatographic (GPC) analysis was performed on a Lab Alliance RI2000 instrument (one column, MIXED-D from Polymer Laboratories) connected with one refractive index detector from Schambeck SFD Gmbh. All GPC analyses were performed using a polymer/DMF solution at a flow rate of 1 mL/min at 70 °C and calibrated with polystyrene standards. Thermogravimetric analysis (TGA) was conducted with a PerkinElmer Pyris 1 TGA. Experiments were carried out on approximately 6–8 mg film samples heated in flowing nitrogen or air (flow rate = 20 $cm^3$/min) at a heating rate of 20 °C/min. DSC analyses were performed on a PerkinElmer Pyris 1 DSC at a scan rate of 10 °C/min in flowing nitrogen (20 $cm^3$/min). Electrochemistry was performed with a CH Instruments 612C electrochemical analyzer. Voltammograms are presented with the positive potential pointing to the left and with increasing anodic currents pointing downwards. Cyclic voltammetry (CV) was conducted with the use of a three-electrode cell in which ITO (polymer films area about 0.5 cm × 1.2 cm) was used as a working electrode. A platinum wire was used as an auxiliary electrode. All cell potentials were taken by using a homemade Ag/AgCl, KCl (sat.) reference electrode. Spectroelectrochemical experiments were carried out in a cell built from a 1 cm commercial UV-visible cuvette using Hewlett-Packard 8453 UV-Visible diode array and Hitachi U-4100 UV-Vis-NIR spectrophotometer. The ITO-coated glass slide was used as the working electrode, a platinum wire as the counter electrode, and a Ag/AgCl cell as the reference electrode. The thickness of the polyamide thin films was measured by alpha-step profilometer (Kosaka Lab., Surfcorder ET3000, Japan). Colorimetric measurements were obtained using JASCO V-650 spectrophotometer and the results are expressed in terms of lightness ($L^*$) and color coordinates ($a^*$, $b^*$).

## Acknowledgements

We gratefully acknowledge the support of this research through the Institute of Nuclear Energy Research, Atomic Energy Council and the National Science Council (NSC98-2113-M-002-005-MY3) in Taiwan, ROC. C. W. Lu of the Instrumentation Center, National Taiwan University, for CHNS (EA) analysis experiments and C. H. Ho of the Instrumentation Center, Department of Chemistry, National Taiwan Normal University, for the measurement of 500 MHz NMR spectrometer are also acknowledged.

## References and Notes

1 (*a*) P. M. S. Monk, R. J. Mortimer and D. R. Rosseinsky, *Electrochromism and Electrochromic Devices*; Cambridge University Press, Cambridge, UK, 2007; (*b*) R. J. Mortimer, *Chem. Soc. Rev.*, 1997, **26**, 147; (*c*) D. R. Rosseinsky and R. J. Mortimer, *Adv. Mater.*, 2001, **13**, 783; (*d*) P. R. Somani and S. Radhakrishnan, *Mater. Chem. Phys.*, 2003, **77**, 117; (*e*) S. Liu, D. G. Kurth, H. Mohwald and D. Volkmer, *Adv. Mater.*, 2002, **14**, 225; (*f*) T. Zhang, S. Liu, D. G. Kurth and C. F. J. Faul, *Adv. Funct. Mater.*, 2009, **19**, 642; (*g*) A. Maier, A. R. Rabindranath and B. Tieke, *Adv. Mater.*, 2009, **21**, 959; (*h*) L. Motiei, M. Lahav,

 

D. Freeman and M. E. van der Boom, *J. Am. Chem. Soc.*, 2009, **131**, 3468; (*i*) P. M. Beaujuge and J. R. Reynolds, *Chem. Rev.*, 2010, **110**, 268.
2 (*a*) U. Bach, D. Corr, D. Lupo, F. Pichot and M. Ryan, *Adv. Mater.*, 2002, **14**, 845; (*b*) A. L. Dyer, C. R. G. Grenier and J. R. Reynolds, *Adv. Funct. Mater.*, 2007, **17**, 1480; (*c*) C. Ma, M. Taya and C. Xu, *Polym. Eng. Sci.*, 2008, **48**, 2224; (*d*) S. Beaupre, A. C. Breton, J. Dumas and M. Leclerc, *Chem. Mater.*, 2009, **21**, 1504.
3 (*a*) T. L. Rose, S. D′Antonio, M. H. Jillson, A. B. Kon, R. Suresh and F. Wang, *Synth. Met.*, 1997, **85**, 1439; (*b*) E. B. Franke, C. L. Trimble, J. S. Hale, M. Schubert and J. A. Woollam, *J. Appl. Phys.*, 2000, **88**, 5777; (*c*) P. Topart and P. Hourquebie, *Thin Solid Films*, 1999, **352**, 243; (*d*) P. Chandrasekhar, B. J. Zay, T. McQueeney, A. Scara, D. Ross, G. C. Birur, S. Haapanen, L. Kauder, T. Swanson and D. Douglas, *Synth. Met.*, 2003, **135–136**, 23.
4 (*a*) S. J. Vickers and M. D. Ward, *Electrochem. Commun.*, 2005, **7**, 389; (*b*) P. F. H. Schwab, S. Diegoli, M. Biancardo and C. A. Bignozzi, *Inorg. Chem.*, 2003, **42**, 6613; (*c*) Y. Qi and Z. Y. Wang, *Macromolecules*, 2003, **36**, 3146; (*d*) S. Wang, E. K. Todd, M. Birau, J. Zhang, X. Wan and Z. Y. Wang, *Chem. Mater.*, 2005, **17**, 6388; (*e*) J. Zheng, W. Qiao, X. Wan, J. P. Gao and Z. Y. Wang, *Chem. Mater.*, 2008, **20**, 6163; (*f*) F. Hasanain and Z. Y. Wang, *Dyes Pigm.*, 2009, **83**, 95; (*g*) P. Shi, C. M. Amb, E. P. Knott, E. J. Thompson, D. Y. Liu, J. Mei, A. L. Dyer and J. R. Reynolds, *Adv. Mater.*, 2010, **22**, 4949; (*h*) G. Sonmez, H. Meng, Q. Zhang and F. Wudl, *Adv. Funct. Mater.*, 2003, **13**, 726; (*i*) G. Sonmez, H. Meng and F. Wudl, *Chem. Mater.*, 2004, **16**, 574; (*j*) M. Li, A. Patra, Y. Sheynin and M. Bendikov, *Adv. Mater.*, 2009, **21**, 1707.
5 M. Robin and P. Day, *Adv. Inorg. Radiochem.*, 1967, **10**, 247.
6 (*a*) C. Creutz and H. Taube, *J. Am. Chem. Soc.*, 1973, **95**, 1086; (*b*) C. Lambert and G. Noll, *J. Am. Chem. Soc.*, 1999, **121**, 8434; (*c*) A. V. Szeghalmi, M. Erdmann, V. Engel, M. Schmitt, S. Amthor, V. Kriegisch, G. Noll, R. Stahl, C. Lambert, D. Leusser, D. Stalke, M. Zabel and J. Popp, *J. Am. Chem. Soc.*, 2004, **126**, 7834.
7 (*a*) G. S. Liou, S. H. Hsiao and T. X. Su, *J. Mater. Chem.*, 2005, **15**, 1812; (*b*) G. S. Liou, S. H. Hsiao, N. K. Huang and Y. L. Yang, *Macromolecules*, 2006, **39**, 5337; (*c*) C. W. Chang and G. S. Liou, *J. Mater. Chem.*, 2008, **18**, 5638; (*d*) C. W. Chang, C. H. Chung and G. S. Liou, *Macromolecules*, 2008, **41**, 8441; (*e*) G. S. Liou, H. Y. Lin and H. J. Yen, *J. Mater. Chem.*, 2009, **19**, 7666; (*f*) G. S. Liou and H. Y. Lin, *Macromolecules*, 2009, **42**, 125; (*g*) H. J. Yen, H. Y. Lin and G. S. Liou, *Chem. Mater.*, (accepted).
8 (*a*) H. J. Yen and G. S. Liou, *J. Polym. Sci., Part A: Polym. Chem.*, 2009, **47**, 1584; (*b*) L. T. Huang, H. J. Yen, C. W. Chang and G. S. Liou, *J. Polym. Sci., Part A: Polym. Chem.*, 2010, **48**, 4747; (*c*) H. J. Yen and G. S. Liou, *Org. Electron.*, 2010, **11**, 299.
9 (*a*) G. S. Liou, S. H. Hsiao, W. C. Chen and H. J. Yen, *Macromolecules*, 2006, **39**, 6036; (*b*) G. S. Liou and H. J. Yen, *J. Polym. Sci., Part A: Polym. Chem.*, 2006, **44**, 6094; (*c*) C. W. Chang, G. S. Liou and S. H. Hsiao, *J. Mater. Chem.*, 2007, **17**, 1007; (*d*) H. J. Yen and G. S. Liou, *J. Mater. Chem.*, 2010, **20**, 9886.
10 (*a*) S. H. Cheng, S. H. Hsiao, T. H. Su and G. S. Liou, *Macromolecules*, 2005, **38**, 307; (*b*) G. S. Liou, S. H. Hsiao and H. W. Chen, *J. Mater. Chem.*, 2006, **16**, 1831; (*c*) G. S. Liou, H. W. Chen and H. J. Yen, *J. Polym. Sci., Part A: Polym. Chem.*, 2006, **44**, 4108; (*d*) G. S. Liou, H. W. Chen and H. J. Yen, *Macromol. Chem. Phys.*, 2006, **207**, 1589; (*e*) G. S. Liou, C. W. Chang, H. M. Huang and S. H. Hsiao, *J. Polym. Sci., Part A: Polym. Chem.*, 2007, **45**, 2004; (*f*) C. W. Chang, H. J. Yen, K. Y. Huang, J. M. Yeh and G. S. Liou, *J. Polym. Sci., Part A: Polym. Chem.*, 2008, **46**, 7937; (*g*) G. S. Liou and C. W. Chang, *Macromolecules*, 2008, **41**, 1667; (*h*) S. H. Hsiao, G. S. Liou, Y. C. Kung and H. J. Yen, *Macromolecules*, 2008, **41**, 2800; (*i*) H. J. Yen and G. S. Liou, *Chem. Mater.*, 2009, **21**, 4062.
11 (*a*) N. Yamazaki, F. Higashi and J. Kawabata, *J. Polym. Sci., Polym. Chem. Ed.*, 1974, **12**, 2149; (*b*) N. Yamazaki, M. Matsumoto and F. Higashi, *J. Polym. Sci., Polym. Chem. Ed.*, 1975, **13**, 1373.
12 Y. Imai, M. Ishida and M. Kakimoto, *High Perform. Polym.*, 2003, **15**, 281.